

# Kinematics of the local universe

## VI. *B*-band Tully-Fisher relation and mean surface brightness

G. Theureau

Observatoire de Paris-Meudon, CNRS URA1757, F-92195 Meudon Principal Cedex, France

Received 7 May 1997 / Accepted 19 September 1997

**Abstract.** Continuing our study of the type dependence of the TF relation, we present a new attempt to reduce the scatter of that relation by using the observed mean surface brightness  $\Sigma$  of galaxies. It is shown that the zero-point of the relation is a continuous function of  $\Sigma$ , well described by a third or fourth degree polynome. Taking this effect into account, the TF scatter decreases by 20 percents, and the uncertainty in the derived TF distances is reduced as well, while the correlation coefficient increases from 0.67 to 0.84 (diameter relation). This study is based on the statistical analysis of the KLUN (Kinematics of the Local Universe) sample of 5271 spiral galaxies, both for diameter and magnitude, direct and inverse TF relations. The absolute calibration is performed using two sets of good cepheid distance measurements: the first one, mostly from the HST programmes, relies on distance moduli generally agreed in the literature, the second one is a subset of objects whose cepheid distance moduli are derived from geometrical distances measured by HIPPARCOS.

The mean surface brightness dependence is first revealed by the inverse relations, and further studied in the direct way through the normalized distance method whose principle was first set by Bottinelli et al. (1986), and a refined form recently applied by Theureau et al. (1997b). As a consequence of the smaller scatter of the resulting TF relation, the extracted unbiased subsample is deeper and contains more objects than in previous studies. The Hubble constant  $H_0$  may thus be estimated from the largest unbiased sample of field galaxies ever used (577 objects reaching velocities as large as  $6000 \text{ km s}^{-1}$ , using the diameter relation). We obtain  $H_0 = 56 \pm 3 \text{ km s}^{-1} \text{ Mpc}^{-1}$  and  $H_0 = 51 \pm 4 \text{ km s}^{-1} \text{ Mpc}^{-1}$  from HST and HIPPARCOS calibrations respectively.

**Key words:** galaxies: spiral – galaxies: distances and redshifts – Cosmology: distance scale

### 1. Introduction

It is now well established that the Tully-Fisher relation in *B*-band depends on galaxy type (Theureau et al. 1997a). This

dependence was shown to be connected to another parameter, the relative proportion of bulge and disc luminosities. This parameter, though not directly observable, is actually known to be correlated with the morphological type,  $K = L_B/L_D$  decreasing from early type spirals to late type or pure disc galaxies (Simien & de Vaucouleurs, 1986). The type dependence can be understood in terms of the relative importance of bulge and disc, and thus practically measured by the bulge to disc luminosity ratio. With a simple model based on reasonable, though rough, assumptions on dark mass, mass to light ratio, HI and molecular gas fraction, this effect is easily explainable and predictable, as it was shown by Theureau et al. 1997a. Confirming previous intuition from Roberts (1978) or Rubin et al. (1985), the dependence appears as a zero-point shift of the TF regression line; the shift with respect to pure disc objects is related to the relative importance of the bulge, either in mass or in luminosity.

Even if this new evidence for a type dependence reduces the dispersion of the TF relations and gives more accurate distances when considering, instead of a common regression, a set of lines shifted according to the type, this result is not quite satisfactory for the following reasons.

Firstly, though well coded, the morphological type is a subjective parameter, which depends sometimes on the catalogue used (see Paturel et al. 1997b), and does not result from a physical measurement. Secondly, types correspond to discrete modes in which the bulge to disc ratio either in luminosity or in mass is highly dispersed when a continuous quantity would be needed to follow the relative dynamical influence of these main components. Finally, the corresponding physical parameter, i.e. the bulge to disc luminosity ratio, is not directly observable: it requires many assumptions and application of theoretical models (Kent 1985, Kodaira et al. 1986). Although, the exponential law seems to give a good fit of the disc photometric profile, the  $r^{1/4}$  law is often criticised in the case of the bulge component (Caon et al. 1993, Capaccioli et al. 1994). In addition, the determination of  $K$  varies from one author to another, depending on the procedure used to separate the two components. And finally, the estimation of  $L_B/L_D$  requires observations of photometric profiles, which are not available for the large sample needed.

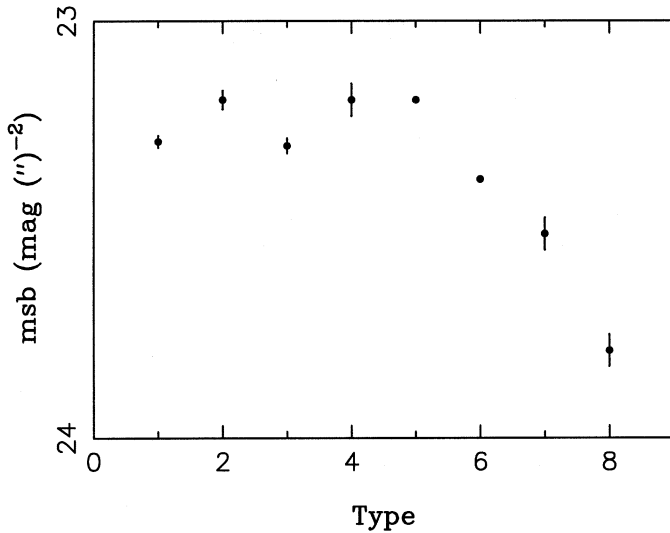


**Fig. 1.** Average mean surface brightness calculated for each morphological type from our KLUN sample. Error bars represent the standard deviation for each type.

Going beyond the type dependence requires an observable and measurable parameter equivalent to the bulge to disc ratio. A first indication could be given by the exponential law ; it is actually possible, using only the shape of the disc profile, to show that this model predicts a bijection between  $K = L_B/L_D$  and the mean surface brightness  $\Sigma$  of a galaxy :

$$K = \frac{\Sigma}{20.48I(0)} - 1$$

where  $I(0)$  is the central surface brightness of a single disc expressed in  $L_{\odot} \text{pc}^{-2}$ .

Our previous work on the type dependence has also shown that the inverse TF residuals (along the  $\log V_m$  axis) are correlated with the mean surface brightness (Theureau et al. 1997a, Fig. 4). It is also well known that late type spirals have generally a lower mean surface brightness than early type ones. This is confirmed using our sample and is shown on Fig. 1 (the description of the sample is summarized in Appendix A).

We remember here that Bothun and Mould (1987) performed one of the first rigorous attempts to use the information contained in the light distribution to minimize the scatter of the TF relation in  $I$ -band. More precisely, they showed that at a fixed line width there is a wide range in surface brightness profiles, which contributes to an additional scatter in the TF relation. Moreover, Bothun (1986) argued, in more physical terms, that these differences in intensity distribution may be related to differences in the shape of the rotation curve, and recommended, as did de Vaucouleurs and collaborators, to use a method of "sosie", that is, to use only galaxies which have similar luminosity profiles as a function of line width. He exhibited also from a sample of pure disc galaxies a correlation between line width and central surface brightness (Fig. 2).

The mean surface brightnesses  $\Sigma$  are calculated using blue magnitudes  $B_t$  and  $D_{25}$  photometric diameters, both corrected

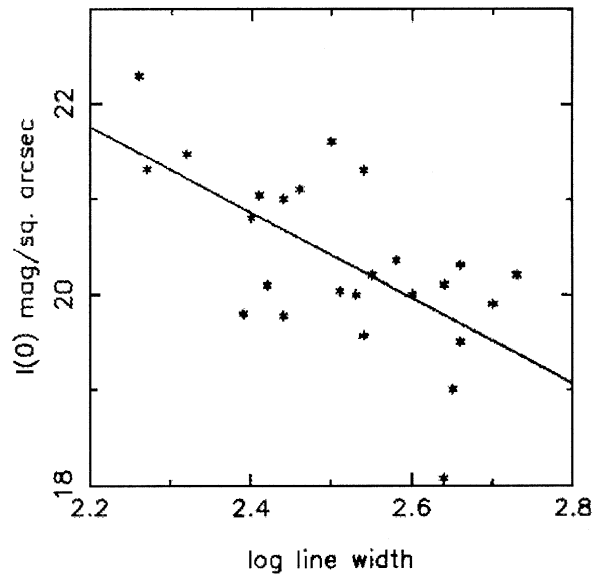


**Fig. 2.** Relationship between line width and central surface brightness for a sample of pure disc galaxies (from Bothun 1986)

for galactic extinction and opacity (see Fouqué&Paturel, 1985 and Bottinelli et al. 1995, respectively). This calculation is based on the assumption that the luminosity  $L_{25}$  emitted within  $D_{25}$  is proportional to the total luminosity  $L_{tot}$  of the galaxy. If this were not verified, our estimation of  $\Sigma$  from the apparent parameters should be biased.

Figs. 3a to 3d show the distribution of the luminosity ratio  $L_{25}/L_{tot}$  as a function of the bulge to disc luminosity ratio  $k$ , the morphological type code, and the intrinsic diameter for the photometrical data published by Kent (1985). Calculations have been made on the basis of the exponential law and the  $r^{1/4}$  law for disc and bulge components respectively.

No correlation is found in first approximation between the ratio  $L_{25}/L_{tot}$  and any of the above parameters; we may then reasonably assume that  $L_{25} = L(r < r_{25})$  represents roughly 90 percents of the total luminosity, with a dispersion of the order of 10 percents.

## 2. The inverse diameter TF relation

As we did for the study of the type dependence, we start here by looking at the behaviour of the inverse diameter TF relation for successive ranges of mean surface brightness. For a fixed absolute diameter  $\log D$ , when the mean surface brightness increases, the luminous mass is expected to increase together with  $\log V_m$ . The inverse relation has the advantage of being insensitive to any selection on apparent diameter or magnitude, then, to be free from the Malmquist bias of the second kind (Schechter 1980, Teerikorpi 1984). Then, the mean surface brightness  $\Sigma$  being a combination of  $D_{25}$  and  $B_t$ , the inverse relation is not affected by the binning of our sample in intervals of brightness. This allows us to use the whole sample (3364 spiral galaxies from Sa to Sdm, within restrictions:  $|b| \geq 15^\circ$ ,  $\log R_{25} \geq 0.07$ ).

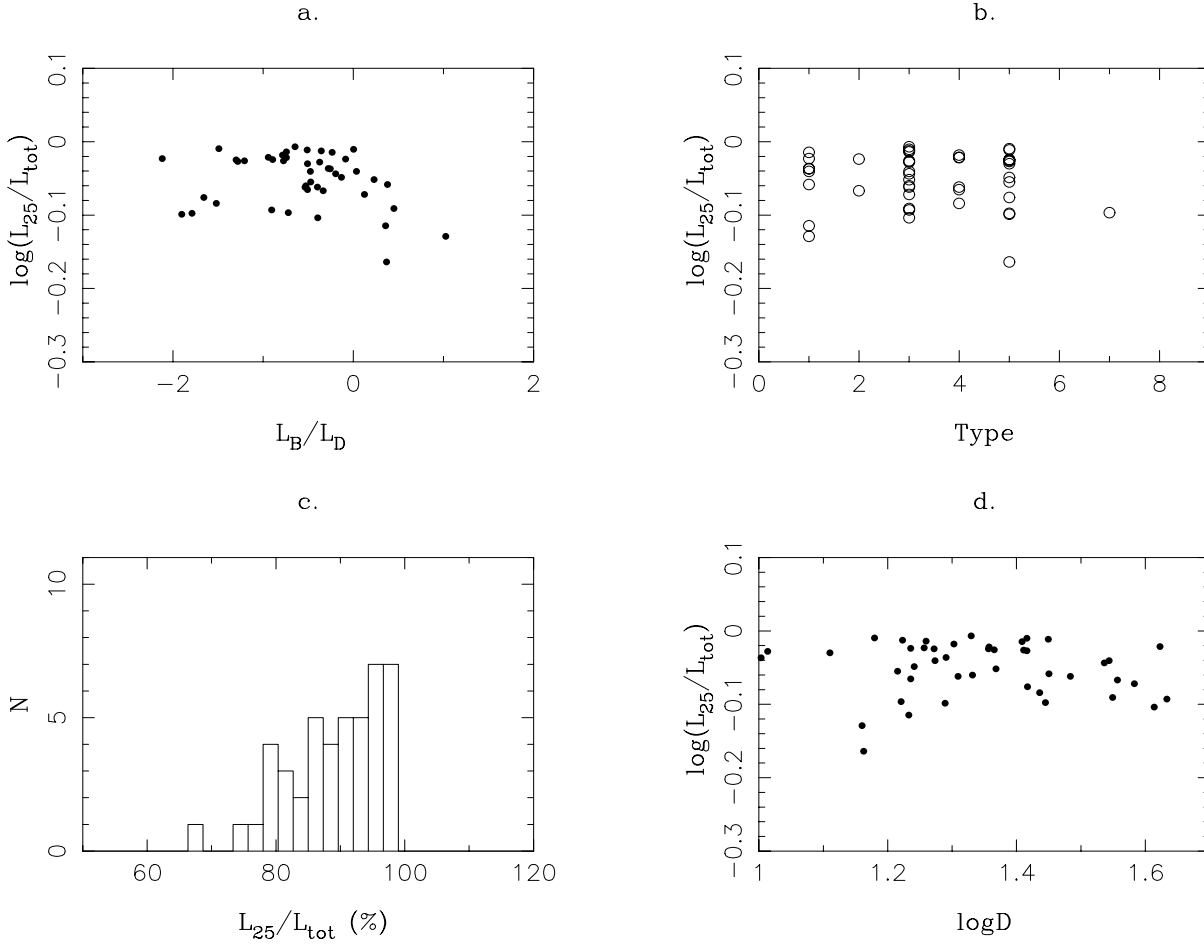


**Fig. 3a–d.** study of  $\log(L_{25}/L_{tot})$  with respect to different observed parameters: **a** relation with bulge to disc luminosity ratio; **b** relation with morphological type; **c** distribution function; **d** relation with the logarithm of absolute diameter

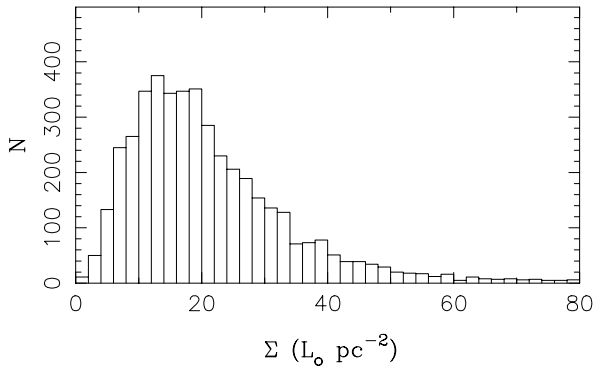


**Fig. 4.** Distribution of the calculated mean surface brightness for our KLUN sample

Most of the objects have their mean surface brightnesses distributed between 0 and 60  $L_{\odot} \text{ pc}^{-2}$  (see histogram Fig. 4); for convenience we restricted our study to this range which has been binned successively in 8, 12, or 16 intervals. The widths of the boxes are then respectively 7.5, 5.0, and 3.8  $L_{\odot} \text{ pc}^{-2}$ .

The slope of the diameter relation is found unchanged along the brightness sequence and close to 0.7. The evidence for this constancy is clear: the dispersion of the derived slopes  $a(\Sigma)$  around the adopted value of 0.7 is very small ( $\sigma=0.02$ , i.e. an error of 3 percents on the slope) and independent of the size of the intervals and of the number of objects in each. The most remarkable, the successive zero-points (the slope being fixed to 0.7) associated with the successive brightness boxes follow a very nice and smooth curve, easily fitted with a polynomial of the third degree. Not only the dispersion is tiny ( $\sigma=10^{-4}$ ), but also the gaps left between two points are filled when the number of intervals is increased or when their size is reduced. This allows us to assume that a continuous effect is linking TF zero-points and mean surface brightness. Figs. 5a, 5b, and 5c show this behaviour for an increasing number of boxes; the curve drawn in Fig. 5a–c is the third degree polynomial evaluated from a least squares fit to the first set of 8 points. Note that the good fit of the curve is not affected when the intervals are reduced. The dispersion of course increases with the number of intervals, because each of them contains less and less objects. We may conclude that this effect is real, and that we are able to

use for each galaxy the best zero-point, fixed by its mean surface brightness. The resulting scatter of the inverse TF relation (along  $\log V_m$  axis) becomes then equal to 0.10, as it was 0.11 when the type was taken into account, or 0.125 when a single relation was used. Starting from this interesting result, we are now going to study the effect on the direct diameter TF relation.

### 3. The direct diameter TF relation

#### 3.1. Specificity

When using the direct Tully-Fisher relation, we have to deal with an additional problem, i.e. the Malmquist bias of the second kind. This bias is connected with the actual situation of the observer who is necessarily working with an instrument limited in sensitivity and thus collects a flux limited sample. The farther he looks, the brighter are the objects he collects. As a result, when distances are estimated from a method such as the direct TF relation, a progressive under-estimation of distances is expected. This effect is very difficult to correct (see Teerikorpi, 1994, Hendry&Simons, 1994, Triay et al. 1994), and analytical solutions require the knowledge of luminosity and  $\log V_m$  distribution functions. In addition, some methods require strong assumptions such as the uniformity of the density, while it is well known that our local universe, at the scale we are interested in, is rather clumpy.

A safe way is to extract from the data an unbiased subsample. We will refer here to the normalized distance method first elaborated by Bottinelli et al. in 1986, and further developed by Theureau et al. (1997b). The main idea is that the luminosity function (or the diameter distribution function) of a class of galaxies, defined by having the same value of  $\log V_m$ , the same inclination (i.e. the same opacity correction), the same galactic latitude (i.e. the same galactic extinction), and in the present paper, the same mean surface brightness  $\Sigma$ , is traced by the sample up to a same limiting distance. Beyond this distance, the luminosity distribution is truncated in its fainter part (galaxies fainter than the limiting magnitude of the sample are not present) and the sample is consequently biased. Moreover, at a given true distance greater than the above limit, the inferred TF distance is equally biased for all the objects of a given class. Thus, if one builds a distance scale in which all the objects are normalized to the same class (which could be understood as a class of "sosies"), the bias will be the same for all the galaxies of the sample which have the same normalized true distance. This normalization allows to extract more easily the unbiased subsample: it appears as a flat part at short normalized distances ( $d_n \leq d_{n,lim}$ ), when  $\log H = V/d_{TF}$  is plotted against  $d_n$ . The method relies on the assumption that the TF scatter  $\sigma_{M_p}$  or  $\sigma_{\log D_p}$  is the same for all the values of  $p = \log V_m$ . Fortunately, there is no evidence for systematic variation of that dispersion with  $p$  (Theureau et al. 1997b) and  $\sigma_{M_p}$  (resp.  $\sigma_{\log D_p}$ ) may be assumed to be constant and equal to the TF relation scatter  $\sigma_{TF}$ .

What is required here is to use a sample which is complete with respect to a limiting diameter or magnitude. We also need a relative distance scale: as in previous papers, we have used the

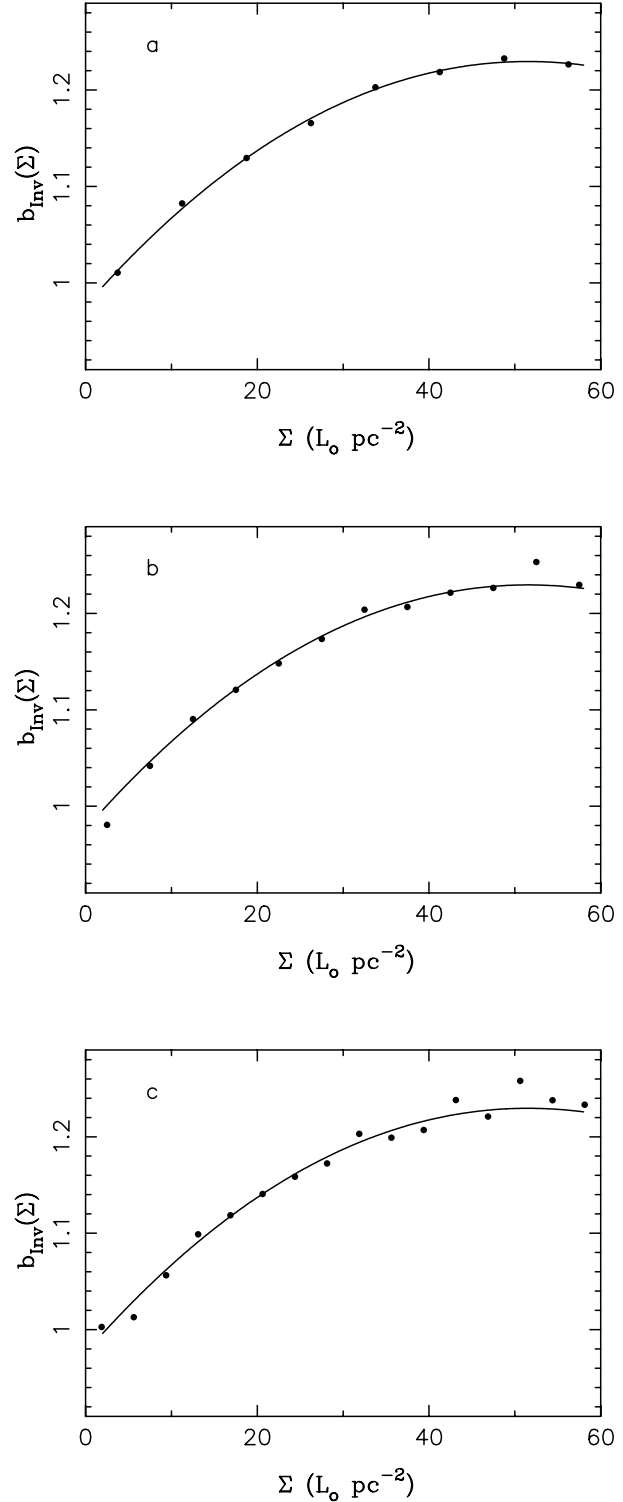


**Fig. 5a–c.** Inverse (diameter) TF zero-point as a function of mean surface brightness for different cut up: **a** 8 intervals; **b** 12 intervals; **c** 16 intervals

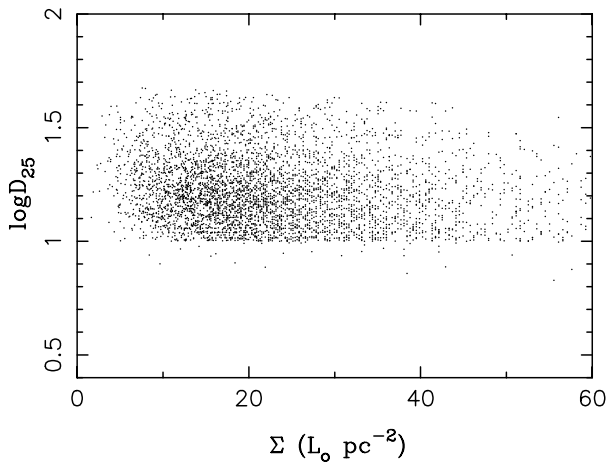


**Fig. 6.** Relationship between apparent diameter  $D_{25}$  and mean surface brightness  $\Sigma$

kinematical distance  $d_{kin}$  built from observed radial velocities corrected for an infall component toward the Virgo cluster. The linear Peebles's infall model has been used, assuming  $v_0 = 150 \text{ km s}^{-1}$  for the infall velocity of the Local Group, and  $(V_0)_{Vir} = 980 \text{ km s}^{-1}$  for the observed mean velocity of Virgo (Mould et al. 1980). See Theureau et al. (1997b) and Ekholm (1996) for detailed discussions of that point.

### 3.2. Application

In practice, the individual  $\log[H_0(i)] = \log[V/d](i)$  are plotted against normalized distance. The calculation of  $H_0(i)$  is based on distances estimated using an iterated TF relation, and the normalized distance scale is built as follows. The average value of  $H_0$  has to be constant as far as the sample remains unbiased. The determination of this plateau sets the limit of the unbiased subsample, which contains, with the normalization method, the largest possible number of points. This method is iterative: it requires as an input the parameters of a TF relation and gives as an output a new and improved TF relation. In order to extract the plateau data as safely as possible, the sample has to be strictly either flux or diameter limited. For that reason, we have especially to pay attention to the way of binning the mean surface brightness. The sample is complete in diameter down to  $\log D_{25} = 1.2$  ( $D_{25}$  in 0.1 arcmin) and this value remains constant whatever the mean surface brightness  $\Sigma$  (Fig. 6 shows the effect of the  $\Sigma$ -selection on the completeness). But this is not the case for magnitudes for which the completeness depends on  $\Sigma$  (see next Sect.).

After 3 iterations a slope of 0.98 is obtained for the diameter relation, with a plateau, i.e. an unbiased sample, containing 877 galaxies (Fig. 7). There again, the slope appears to be quite stable (rms=0.07, i.e. an error of 7 percents in the slope) and the zero-point shift with  $\Sigma$  (in the range [0. ; 55.]) is well evidenced (Figs. 8a and 8b). Outside this  $\Sigma$ -range, the sample is too small to give a confident regression. A fourth degree polynome is used for the fit, and as it was seen above for the inverse relation, it

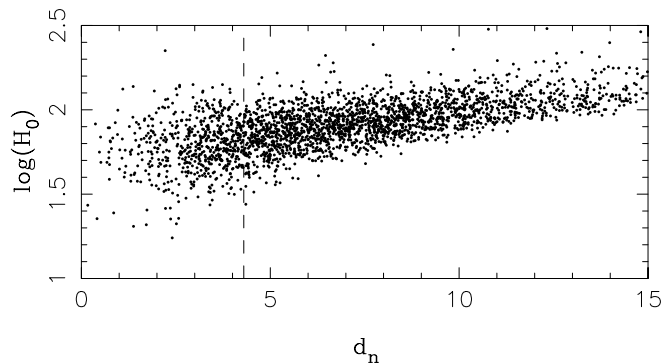


**Fig. 7.** Normalized distance diagram  $\log H_0$  vs.  $d_n$  and visualization of the plateau

is independent of the number of  $\Sigma$ - intervals. Fig. 9 shows the normalized TF relation obtained when moving the points to the same zero-point according to their mean surface brightness. The dispersion of the diameter TF relation is now reduced to 0.125.

## 4. The case of the magnitude TF relations

We have seen previously that at a fixed given diameter  $D$ , the maximum of rotational velocity increases when the mean surface brightness  $\Sigma$  is increasing (one may note that the total luminosity increases also). This is normally expected when considering that, at a fixed absolute diameter  $D_{25}$ , the size of the disc is also fixed. Consequently, when the mean surface brightness increases, the luminous mass increases essentially within the bulge component and the situation is the same as for the type dependence (see Theureau et al. 1997a).

The situation is more complicated when considering the magnitude TF relations. If we fix the absolute magnitude  $M_{B_t}$ , and select objects with increasing  $\Sigma$ , the absolute diameter is expected to decrease as  $\Sigma^{-1/2}$  and we have to deal with two opposite effects: an increasing mass of the bulge and a decreasing mass of the disc, and it is difficult to predict in which direction  $\log V_m$  will change. In fact, when calculating the inverse slope and the corresponding zero-points  $b(\Sigma)$  from the method described in Sect. 2, there is a trend of the zero-point to decrease with increasing  $\Sigma$ , contrarily to the case of the diameter inverse TF relation.

In the case of the direct relation, as said previously (Sect. 3), the use of the normalized distance method to select an unbiased subsample requires the total parent sample to be strictly flux limited, i.e. to be complete in apparent magnitude ( $B_t$ ). It is clear that the cut off in magnitude depends on the mean surface brightness; it is then necessary to take this effect into account in the normalized distance formula, using a supplementary term of the form:

$$10^{0.2(m_0 - m_{lim}(\Sigma))}$$

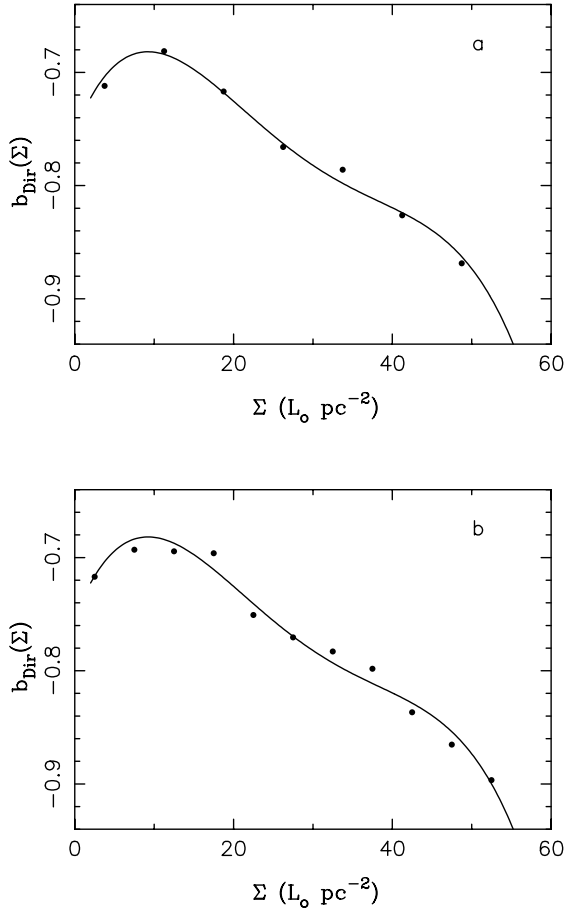


**Fig. 8a and b.** Direct (diameter) TF zero-point as a function of mean surface brightness for different binning: **a** 8 intervals; **b** 12 intervals

In the ideal case, it is possible to derive the function  $m_{lim}(\Sigma)$  for a sample complete down to a given diameter limit  $D_{lim}$  when  $\Sigma$  is calculated from  $B_t$  and  $\log D_{25}$  as follows:

$$\Sigma = 10^{-0.4[B_t + 5(\log D_{25} + \log 6) + 2.5 \log \frac{\pi}{4}] + 10.58}$$

where  $D_{25}$  is expressed in arcmin and  $\Sigma$  in  $L_{\odot} \text{ pc}^{-2}$

$$\Sigma = \frac{10^{-0.4B_t} 10^{10.58}}{D_{25}^2 9\pi}$$

then, if  $D_{25} \geq D_{lim}$  ( $=1.6$  arcmin), we get

$$B_t \leq m_{lim} = -2.5 \log \left( D_{lim}^2 \Sigma \frac{9\pi}{10^{10.58}} \right)$$

However, the selection depending also on extinction and opacity, this formula is only able to provide us with the shape of the selection function in the  $B_t$  vs.  $\Sigma$  diagram. In order to fix the zero-point of this function, we have estimated the magnitude limit for a series of brightness ranges, by measuring the cut-off in  $\log D_{25}$  vs.  $B_t$  diagrams. The corresponding points  $m_{lim}(\Sigma_i)$  are seen as filled squares in Fig. 11, and their general trend follows well the shape of the above function (full line) and allows

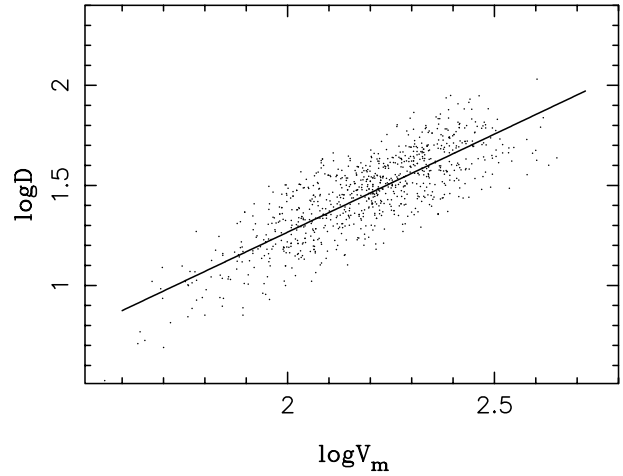


**Fig. 9.**  $\Sigma$ -normalized direct diameter TF relation

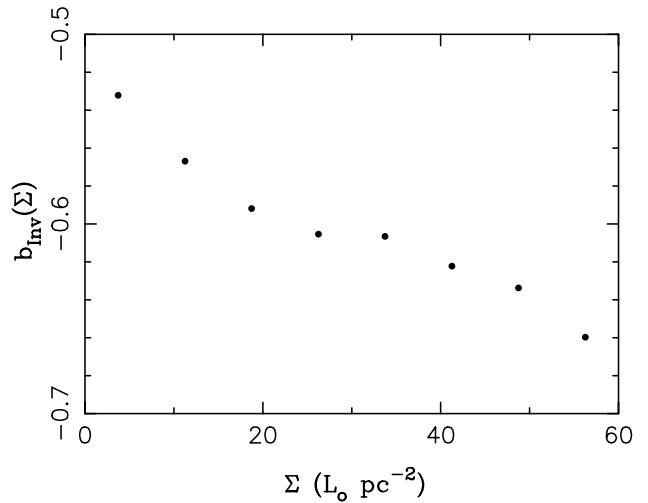


**Fig. 10.** Inverse (magnitude) TF zero-point as a function of mean surface brightness, for a constant slope  $a = 0.135 \pm 0.005$

us to fix a reliable zero-point. This selection function can now be applied to the sample, in order to extract a safe, strictly flux limited, subsample. Following the method described in Sect. 3, we derived an unbiased TF slope on the basis of an unbiased subsample containing 1171 objects. The corresponding relative zero-point  $b(\Sigma)$  is plotted in Fig. 12. The last point outside the polynomial fit has no weight, being calculated from less than 20 galaxies. We thus adopt the dashed line as the  $b(\Sigma)$  function.

## 5. Absolute TF zero-points and $H_0$ therefrom

### 5.1. Calibration

To get an absolute zero-point function  $b(\Sigma)$  for the TF relations, we need a sample of primary calibrators. We first used the same set of cepheid distances as in our previous KLUN analysis (see Table 1 in Theureau et al. 1997b). Its statistical properties were studied in detail: no evidence was found for any correlation of absolute diameter, absolute magnitude,  $\log V_m$ , and diameter or

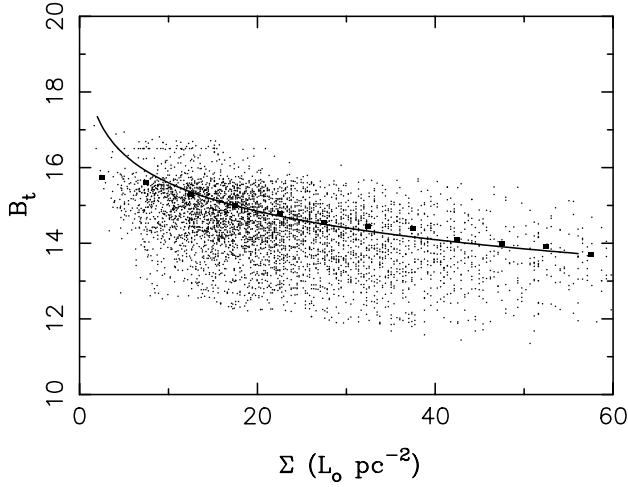


**Fig. 11.** Relationship between apparent  $B$ -magnitude limit and mean surface brightness (see text)

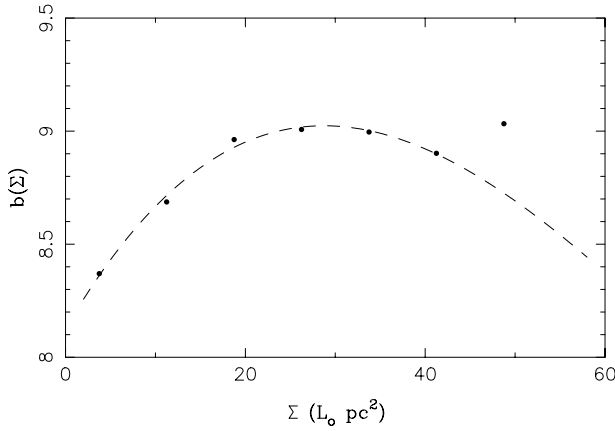


**Fig. 12.** Direct (magnitude) TF zero-point as a function of mean surface brightness: the dashed line represents the polynome adopted

magnitude TF residuals with the distance. The calibrator sample thus appears statistically equivalent to a volume limited sample and would not introduce any bias in the final results. We recall here that very face-on galaxies were rejected because the  $\log V_m$  estimation is uncertain, due to the contribution of internal dispersion to the width of the 21-cm line and to the large relative error on inclination. Very peculiar objects such as the Sombrero ( $M104$ ) and very late types ( $T \geq 9$ ) have also been excluded from the cepheid distance sample. Within these restrictions, we are left with 15 objects. Following Ekholm (1996) and Theureau et al. (1997b) we have assumed that the TF slope has been correctly determined using our large sample of field galaxies; this is indeed well verified, field galaxies and calibrators giving approximately the same value ( $\Delta a/a < 2\%$ ). The relative zero-point function  $b(\Sigma)$  is then also assumed to be the same: it just needs an absolute calibration. In practice, the calibrating galaxies are normalized to the same mean surface brightness arbitrarily fixed to  $\Sigma = 10 L_\odot \text{ pc}^{-2}$ , and the corresponding zero-point  $b_D(10)$  is estimated for an adopted slope  $a_D = 0.98$ . The full line in Fig. 13 shows the result of that calibration which

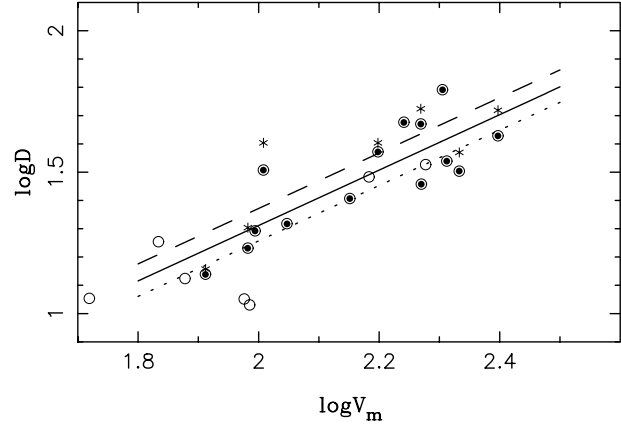


**Fig. 13.** Absolute calibration of the diameter TF relation using: (1) a set of 15 good cepheid distances from literature (dotted circles, full line), (2) an extended sample of 23 group distances (circles, dotted circles, dotted line), and (3) a subset of 8 objects with distance moduli based on HIPPARCOS parallaxes (stars, dashed line)

gives  $b_D(10) = -0.6486$ . The adopted  $\Sigma$ -dependent direct TF relation is then the following:

$$\log D = 0.98 \log V_m + b_D(\Sigma)$$

where

$$b_D(\Sigma) = 0.7864 + (1.78410^{-2})\Sigma - (1.38610^{-3})\Sigma^2 + (3.38110^{-5})\Sigma^3 - (2.83810^{-7})\Sigma^4$$

( $\Sigma$  is expressed in  $L_\odot \text{ pc}^{-2}$ ,  $D$  in kpc, and  $V_m$  in  $\text{km s}^{-1}$ )

The equivalent results for the magnitude relation are the following:

$$-M = 5.13 \log V_m + b_M(\Sigma)$$

where

$$b_M(\Sigma) = 8.571 + (6.82910^{-2})\Sigma - (1.49210^{-3})\Sigma^2 + (7.04710^{-6})\Sigma^3$$

As in Theureau et al. (1997b), we also made the calibration with an extended sample containing group distances (i.e. objects in a group where cepheids were observed). As expected from the previous study, this sample provides us with a slightly shorter distance scale (dotted line).

The HIPPARCOS calibration (objects marked with a star in Fig. 13) gives a distance scale 10% longer. This was expected from Paturel et al. (1997c), and Feast and Catchpole (1997). It should be noted that this sample contains fewer galaxies than the previous ones, because we selected only objects for which an information on colour was available (i.e. photometry in at least two different frequency bands), to achieve the careful calibration of the Period-Luminosity-Colour relation, which takes into account colour, metallicity, and also biasing effects (Paturel et

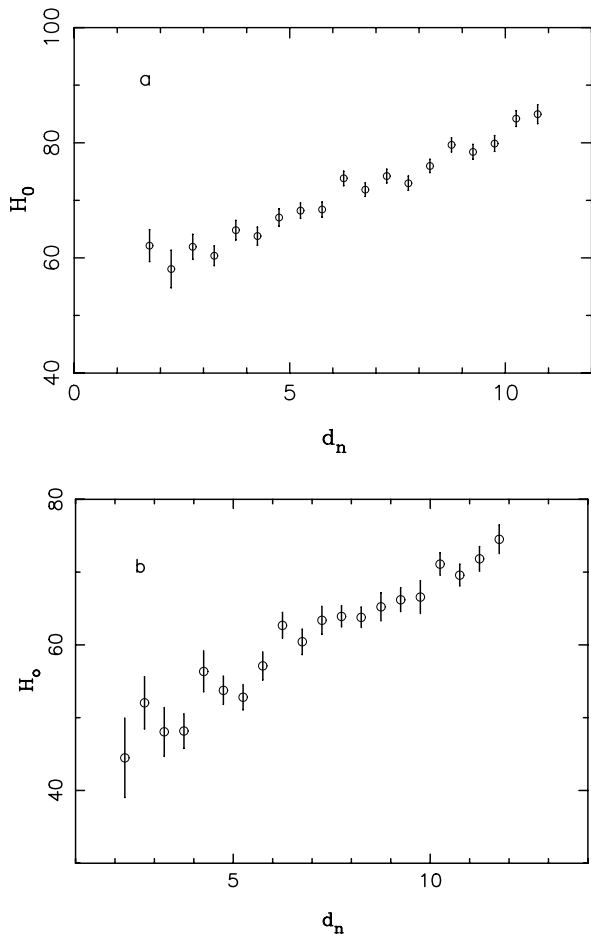


**Fig. 14a and b.** Estimated  $H_0$  for increasing normalized distance range: **a** using the diameter relation; **b** using the magnitude relation

al. 1997c). However, due to larger uncertainties on cepheid distances induced by parallaxes measurement errors, and the less numerous calibrators available, the uncertainty on the TF zero point, and consequently the external error on  $H_0$ , is increased by 40% in the case of the HIPPARCOS calibration.

### 5.2. Value of $H_0$

The Hubble constant  $H_0$  is obtained from the objects selected in the unbiased plateau region, defined according to the normalized distance method. The estimated  $H_0$  is then equal to  $10^{(\log H_0(i))}$ , where the individual  $\log H_0(i)$  are considered in first approximation normally distributed around  $\log H_0$ . In fact, we assume that the bias which could result from a non gaussian distribution of the velocities around  $\log V_{cosmic}$  is negligible, except for the nearest part of our sample where peculiar motions and local bulk flows such as the so-called Local Anomaly (Faber&Burstein, 1988) make uncertain the determination of the cosmological velocity. We have then excluded the closest objects (within  $700 \text{ km s}^{-1}$  in observed radial velocity) from the calculation of the Hubble constant; this concerns at least 60 galaxies. Fig. 14a shows the evolution of  $H_0$  with increasing normalized distance when the diameter relation is used:  $H_0$

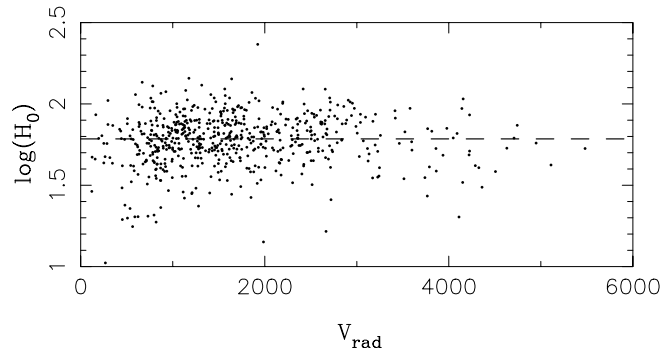


**Fig. 15.** Distribution of individual  $\log H_0 = \log(V/d_{TF})$  in real space

is constant up to  $d_n = 4.5$  and starts to grow up very steeply after; this is the expected effect of the Malmquist bias of the second kind. The plateau region corresponds to the normalized distance range  $[0, 4.5]$ , and, excluding the 60 closest objects ( $V_{obs} \leq 700 \text{ km s}^{-1}$ ), we obtained  $H_0 = 61.0 \pm 4 \text{ km s}^{-1} \text{ Mpc}^{-1}$  by using 577 spiral galaxies from the unbiased domain. The corresponding result for the magnitude relation (Fig. 14b) is  $H_0 = 52.5 \pm 6 \text{ km s}^{-1} \text{ Mpc}^{-1}$  for  $d_n \leq 6.0$  (598 galaxies). These two values are consistent within  $2\sigma$  with  $H_0 = 56 \pm 3 \text{ km s}^{-1} \text{ Mpc}^{-1}$ . The HIPPARCOS calibration, which is more robust because based on geometrical distances, leads to  $H_0 = 51 \pm 4 \text{ km s}^{-1} \text{ Mpc}^{-1}$ .

## 6. Summary and conclusion

This study leads to a number of improvements. First of all, the plateau region is better defined and the distance where the Malmquist bias begins to have an influence is more clearly seen than in previous studies. The corresponding unbiased subsample used to calculate  $H_0$  contains also significantly more objects: nearly 600 galaxies to be compared to only 400 when the type dependence was taken into account. The more extended plateau ( $V_{lim} = 6000 \text{ km s}^{-1}$ , see Fig. 15) allows to study farther regions; this is a direct consequence of the smaller dispersion obtained from the mean surface brightness method :  $\sigma = 0.125$  instead of 0.148 when the type effect is considered, or 0.155 when a single regression is considered (direct diameter relation);  $\sigma = 0.56$  instead of 0.6, or 0.62 (direct magnitude relation). This results in an improvement of 45 % on the determination of  $H_0$  (internal error). In addition, the stability of both the direct and the inverse slopes is now firmly established; and the clear zero-point variation, both in inverse or direct relations, provides us with a reliable tool. The correlation coefficient of the regression is also significantly improved: for the diameter relation, it reaches now 0.84 in comparison with 0.71 when the type effect was taken into account, or to 0.67 when no dependence was considered (resp. 0.73, 0.76, and 0.83 for the magnitude relation). This is probably the most brilliant evidence for the validity of the results and the reality of the mean surface brightness dependence. We have now in hand a better and more powerful tool enabling us a reliable study of the peculiar velocity field of spiral galaxies in our local universe, within a radius of about 80

Mpc. Finally, the first but fundamental application of this new TF relation, is an estimation of the Hubble constant  $H_0$  which has never before been calculated from such a large number of bias-free objects. In addition, the absolute calibration, which is based on geometrical distances (HIPPARCOS parallaxes of cepheids), provides us with a firm result.

It should be noted that the above method assumes that the covariance of  $\Sigma$  and  $\log V_m$  is a constant, and doesn't depend for example on the morphological type. In fact, a variation of  $cov(\Sigma, \log V_m)$  with the type might introduce variations of the derived slope and then contribute to the observed TF scatter. A next step could be to build, from the different values of  $cov(\Sigma, \log V_m)(T)$ , a normalized  $\Sigma_n$  independent of  $\log V_m$ . In this way, we would take into account all the observed parameters of the galaxies sampled for estimating their distance. However, this effect is rather minor and we leave this point for a further statistical study of Tully-Fisher distance estimation.

The above results offer a great progress in the use of the Tully-Fisher relation as a distance indicator. The study of the type dependence (Theureau et al. 1997a) already showed that the rather important scatter of the Tully-Fisher relation can be reduced by considering additional parameters. Substituting the mean surface brightness to the type brings now a substantial improvement. Building an optimum distance indicator, using all the available observables, may be realistic. Despite the richness of  $B$ -band photometric catalogues, many recent authors favour now the use of  $K$  or  $I$  bands, for the simple reason that the TF scatter appears smaller. Our study gives us the hope to lead the  $B$ -band Tully-Fisher relations to the same level of quality as it is in  $K$  and  $I$  bands, while keeping the advantage of working with very large samples of galaxies (see Appendix B).

*Acknowledgements.* I would like to thank Lucette Bottinelli, Lucienne Gouguenheim, Pekka Teerikorpi, and Stephane Rauzy for many interesting discussions during the preparation of this paper. I have made use of data from the Lyon-Meudon Extragalactic Database (LEDA) compiled by the LEDA team at the CRAL-Observatoire de Lyon (France).

## Appendix A: the KLUN sample

KLUN is the sample of spiral galaxies that we have studied and used all along the series of papers the "Extragalactic Data Base" (Paturel et al. 1989, Bottinelli et al. 1990, Paturel et al. 1991a, 1991b, 1994a, Bottinelli et al. 1995) and "Kinematics of the local universe" (Paturel et al. 1994b, Bottinelli et al. 1992, 1993, Di Nella et al. 1996, Theureau et al. 1997a, 1997b). It contains 5271 objects having measured isophotal diameter  $D_{25}$ , HI line width, radial velocity, and also partially (4577)  $B$ -magnitudes. The sample is diameter limited, complete down to  $D_{25} = 1.6$  arcmin and covers the type range Sa-Sdm ( $T=1-8$ ). The data are extracted from LEDA and have been reduced to a standard and common system according to Paturel et al. (1991, 1997a, 1997b) for photometric data and Bottinelli et al. (1990) for HI data. Isophotal  $D_{25}$  diameters and apparent  $B$ -magnitudes are corrected for galactic extinction according to Fouqué&Paturel (1985), and for inclination effect (i.e. opacity effect) in agreement with Bottinelli et al. (1995). HI line widths, reduced to

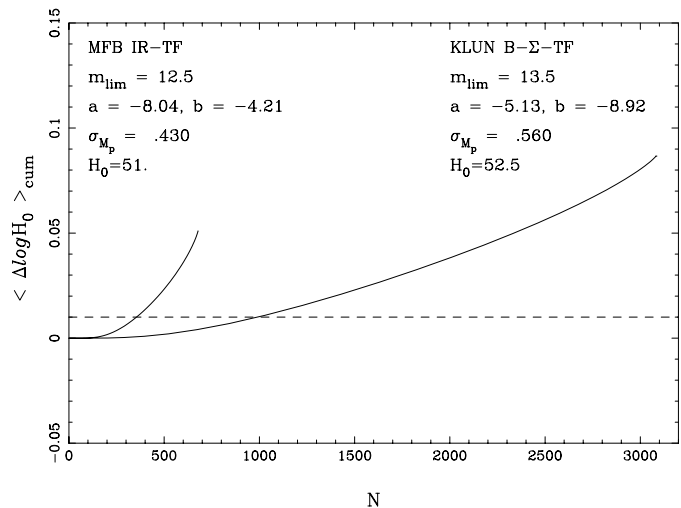


**Fig. 16.** Cumulative error of  $\langle \log H_0 \rangle$  for different number of galaxies used for the plateau, using the MFB sample and the KLUN sample. The completeness limits and TF parameters used for the theoretical curves are listed above each curve. The dashed line represents the limiting value  $\langle \Delta \log H_0 \rangle = 0.01$ . The magnitude complete subsamples contain respectively 678 (MFB) and 3082 (KLUN) galaxies. Formulae used to derive these curves are given by Theureau et al. (1997b).

the standard levels of 20% and 50%, are corrected for internal velocity dispersion according to Tully&Fouqué (1985). Heliocentric radial velocities are corrected to the centroid of the Local Group according to Yahil et al. (1977). The normalized distance method (Sect. 3) is based on a kinematical distance scale  $d_{kin}$  built assuming an infall velocity of the Local Group toward the Virgo cluster  $v_0 = 150 \text{ km s}^{-1}$  and an observed radial velocity of Virgo  $(V_0)_{Vir} = 980 \text{ km s}^{-1}$  (Mould et al. 1980) and using Peebles's linear infall model (1976). Galaxies close to the galactic plane ( $|b| \leq 15^\circ$ ) are excluded (because of too large uncertainties in the galactic extinction correction, see Paturel et al. 1997b). Face-on galaxies ( $\log R_{25} < 0.07$ ) are excluded because of the larger error on  $\log V_m$ . And finally, we excluded also too close objects and those belonging to the "triple value region" around the Virgo core because of the large uncertainties on their kinematical distance. After these restrictions, we are left with 3622 galaxies having both diameter and magnitude measurements.

## Appendix B: comparison between IR and B-bands results on $H_0$

For direct comparison, we applied our normalized distance method to the Mathewson et al. (1992) catalogue (MFB sample), estimated therefrom the  $IR$ -TF parameters, and determined independently the Hubble constant (see Theureau et al. 1998). Our main results are the following:

- This sample was shown to be complete in magnitude up to  $I=12.5$  mag.

- From an observed dispersion of 0.43 mag (field galaxies), we confirmed the intrinsic  $I$ -band TF scatter to be close to 0.3 mag.
- An unbiased subsample of 190 field galaxies is available, extending approximately on the same range of redshift as the KLUN unbiased subsample described above.

The Hubble constant has been calculated from this subsample and an absolute calibration provided by cepheid distances. Fig. 16 shows the effect of the bias on  $H_0$  as a function of the number of objects included in the normalized distance limited subsample (for more details see Fig. 11 in Theureau et al. 1997b). The two curves correspond respectively to the bias behaviour for the two samples (MFB and KLUN) using the  $I$ -band TF relation and the  $B$ -band  $\Sigma$ -dependent TF relation respectively. For keeping  $\langle \Delta H_0 \rangle \leq 0.01$ , for example, the unbiased subsample should not contain more than  $\simeq 300$  objects for the MFB sample, or more than  $\simeq 1000$  objects for the KLUN sample, leading to a factor  $\sqrt{\frac{N_{KLUN}}{N_{MFB}}} \simeq 1.8$  on the  $H_0$  uncertainty between the two determinations. Though the TF scatter in  $I$ -band is 30% smaller than in  $B$ -band,  $H_0$  is determined with a 25-30% better accuracy with the KLUN sample than with the MFB sample.

## References

- Bosma, A., Freeman, K., 1993, AJ 106, 1394  
 Bottinelli, L., Gouguenheim, L., Fouqué P., Patuarel, G., 1990, A&AS 82, 391  
 Bottinelli, L., Durand, N., Fouqué P. et al., 1992, A&AS 93, 173  
 Bottinelli, L., Durand, N., Fouqué P. et al., 1993, A&AS 102, 57  
 Bottinelli, L., Gouguenheim, L., Patuarel, G., Teerikorpi, P., 1995, A&A 296, 64  
 Bothun, G., 1986, in Galaxy Distances and Deviation from Universal Expansion, eds. B.F. Madore and R.B. Tully, Reidel Publishing Company, 87-92  
 Bothun, G., Mould, J., 1987, ApJ 313, 629  
 Bottinelli, L., Gouguenheim, L., Patuarel, G., Teerikorpi, P., 1986, A&A 156, 157 (BGPT86)  
 Caon, N., Capaccioli, M., D’Onofrio, M., 1993, MNRAS 265, 1013  
 Capaccioli, M., Caon, N., D’Onofrio, M., 1995, Astrophys. Lett. Comm. 31, 169  
 Di Nella, H., Patuarel, G., Walsh, A. et al, 1996, A&ASS 118, 311  
 Ekholm, T., 1996, A&A 308,7  
 Faber, S., Burstein, D., 1988, in Large Scale Motions in the Universe, eds. V. Rubin and G. Coyne, Princeton University Press, Princeton, p.11 5  
 Feast, M., Catchpole, R., 1997, MNRAS (in press)  
 Fouqué P., Patuarel, G., 1985, A&A 150, 192  
 Kent, S.M., 1985, ApJS 59, 115  
 Kodaira, K., Watanabe, M., Okamura, S., 1986, ApJS 62, 703  
 Mathewson, D.S., Ford, V.L., Buchhorn, M., 1992, ApJS 81, 413  
 Mould, J. et al. 1980, ApJ 238, 458  
 Patuarel, G., Fouqué, P., Bottinelli, L., Gouguenheim, L., 1989, A&AS 80, 299  
 Patuarel, G., Fouqué, P., Buta, R., Garcia, A., 1991a, A&A 243, 319  
 Patuarel, G., Petit, C., Kogoshvili, N. et al., 1991b, A&AS 91, 371  
 Patuarel, G., Bottinelli, L., Gouguenheim, L., 1994a, A&A 286, 768  
 Patuarel, G., Bottinelli, L., Di Nella, H. et al., 1994b, A&A 289, 711  
 Patuarel, G., Garnier, R., Petit, C., Marthinet, M., 1997a, A&A 311, 12  
 Patuarel, G., Andernach, H., Bottinelli, L. et al., 1997b, A&ASS 124, 109  
 Patuarel, G., Lanoix, P., Garnier, R. et al., 1997c, HIPPARCOS Venice’97 symposium, ESA SP-402 in press  
 Peebles, P., 1976, ApJ 205, 318  
 Roberts, M., 1978, AJ 83, 1026  
 Rubin, V.C., Burstein, D., Ford, Jr W.K., Thonnard, N., 1985, ApJ 289,81  
 Schechter, P.L., 1980, AJ 85, 801  
 Simien, F., Vaucouleurs, G. de, 1986, ApJ 302, 564  
 Teerikorpi, P., 1984, A&A 141, 407  
 Teerikorpi, P., 1995, Astrophys. Lett. Comm. 31, 263  
 Theureau, G., Hanski, M., Teerikorpi, P. et al., 1997a, A&A 319, 435  
 Theureau, G., Hanski, M., Ekholm, T. et al., 1997b, A&A 322, 730  
 Theureau, G. et al., 1998, A&A in preparation  
 Triay, R., Lachièze-Rey, M., Rauzy, S., 1994, A&A 289, 19  
 Tully, B., Fouqué, P., 1985, ApJS 58, 67  
 Yahil, A., Tammann, G., Sandage, A., 1977, ApJ 217, 903